

# Numerical study of aerodynamic forces on trains in crosswind using LES turbulence model

Muhammad Bilal WARIS<sup>a</sup>, Takeshi ISHIHARA<sup>b</sup>,  
Muhammad Waheed SARWAR<sup>c</sup> & Yozo FUJINO<sup>d</sup>

<sup>a,b,c</sup> Institute of Engineering Innovation, School of Engineering, The University of Tokyo,  
2-11-16, Yayoi, Bunkyo-ku, Tokyo 113-8656, Japan

<sup>d</sup> Department of Civil Engineering, The University of Tokyo,  
7-3-1, Hongo, Bunkyo-ku, Tokyo 113-8656, Japan

**ABSTRACT:** Crosswind stability is a major concern for modern lightweight trains. Aerodynamic coefficients are measure of forces acting on trains in crosswinds, which mainly depend upon the train shape and infrastructure configuration. In previous numerical studies several simplifications in geometric details are considered, this paper intends to show the effect of such simplifications on the aerodynamic characteristics. The paper also considers the effect of such simplification on underbody flow and extent of detail required for more realistic flow structure in the numerical domain. Further, the influence of embankment on aerodynamic characteristics and change in flow mechanism is studied. In the end a comparison of LES turbulence model with  $k-\varepsilon$  models is presented.

**KEYWORDS:** Train, Crosswind, Aerodynamics, Geometry, Infrastructure, LES.

## 1 INTRODUCTION

Crosswind stability of train is a major issue in the field of railway transportation, which strives to use light vehicles to improve fuel efficiency and reduce track maintenance. Crosswinds have caused several accidents and are responsible for numerous operational delays. Suzuki et al. [1] reports that nearly 29 wind-induced train derailment accidents have took place in Japan only since the start of the transport service. In most of the cases, crosswind was found to be the reason of derailment. Some recent examples of such incidence are the derailment in Yamagata prefecture, northern Japan on 25 December 2005 and in Nobeoka, Miyazaki prefecture, southern Japan on 17 September 2006.

Aerodynamic characteristics are the most important and governing parameter in the evaluation of train stability in crosswind. These characteristics have been found to depend upon several parameters that include train shape, infrastructure configuration, boundary layer etc [1].

Suzuki et al [1] conducted experiments to evaluate train shape and infrastructure effects on aerodynamic coefficients, and quantifies their dependence on these parameters. Chiu [2] carried out experiments on an idealized train model to study the effect of yaw angle on the vortex shedding mechanism and reported that pressure distribution is essentially two-dimensional at sections away from the nose. Chiu [3,4] then used two- and three-dimensional vortex panel method to predict the pressure distributions with reasonable accuracy for the idealized shape. However, these experimental studies do not provide much information about flow structure and pressure distributions to properly understand the mechanism for realistic train models.

On the other hand, CFD have been used to understand several aerodynamic and engineering problems. Ishihara [5] have provided with good quantitative agreement with experiments for aerodynamic forces acting on a rectangle. However the field of vehicle aerodynamics still lacks use of CFD. Meada [6] has used a two-dimensional numerical model to study effect of bridge on the aerodynamic coefficients of trains in crosswind. Since, a two dimensional model is not able to properly consider attachment details and cannot provide proper flow mechanism, therefore it is not suitable to evaluate aerodynamic characteristics. Khier [7] used simplified numerical model for the German InterRegio coach to investigate flow structure for various yaw angles, providing detailed information about flow structures at various angles. However, ignoring attachments can be of great significance on the flow structure. L. Cléon, et al. [8] has compared experiments with CFD using  $k-\varepsilon$  model and shows that  $k-\varepsilon$  does not provide good results for the case of train on embankment.

This paper intends to clarify the effect of geometric simplification, adopted during numerical modeling of trains, on aerodynamic characteristics using the LES turbulence model. The significance of model detailing and extent of detail required to obtain accurate aerodynamic characteristics is investigated. Secondly, the influence of embankment on aerodynamic characteristics and change in flow pattern and pressure distributions is considered. Finally, the paper also looks into the applicability and shortcomings of  $k-\varepsilon$  models through a comparison with LES. Section 2 explains numerical model, governing equation, boundary conditions and modeling details. Section 3 provides results and discussion of the numerical computation and in section 4 has conclusions.

## 2 NUMERICAL MODEL

Large Eddy Simulation (LES) turbulence model is used in this study because of its ability to capture turbulence characteristics that are unsteady and three dimensional in nature.

### 2.1 Governing equations & Turbulence model

The governing equations employed in LES model are obtained by filtering the time-dependent Navier-Stokes equations as follows:

$$\frac{\partial \rho \bar{u}_i}{\partial x_i} = 0, \quad \frac{\partial}{\partial t}(\rho \bar{u}_i) + \frac{\partial}{\partial x_j}(\rho \bar{u}_i \bar{u}_j) = \frac{\partial}{\partial x_j} \left( \mu \frac{\partial \bar{u}_i}{\partial x_j} \right) - \frac{\partial \bar{P}}{\partial x_i} - \frac{\partial \tau_{ij}}{\partial x_j} \quad (1)$$

where ' $\bar{u}_j$ ' and ' $\bar{P}$ ' are filtered mean velocity and filtered pressure respectively, ' $\rho$ ' is density, and ' $\tau_{ij}$ ' is sub-grid-scale stresses, an unknown from the filtering operations modeled as:

$$\tau_{ij} = -2\mu_t \bar{S}_{ij} + \frac{1}{3} \tau_{kk} \delta_{ij}, \quad \bar{S}_{ij} \equiv \frac{1}{2} \left( \frac{\partial \bar{u}_i}{\partial x_j} + \frac{\partial \bar{u}_j}{\partial x_i} \right) \quad (2)$$

where ' $\mu_t$ ' is sub-grid-scale turbulent viscosity, and ' $\bar{S}_{ij}$ ' is the rate-of-strain tensor.

Smagorinsky model is used for the sub-grid-scale turbulent viscosity ' $\mu_t$ ' which is given as:

$$\mu_t = \rho L_s^2 |\bar{S}| = \rho L_s \sqrt{2\bar{S}_{ij}\bar{S}_{ij}}, \quad L_s = \min(\kappa\delta, C_s, V^{1/3}) \quad (3)$$

where ' $L_s$ ' is the mixing length of sub-grid-scales, ' $\kappa$ ' is the von-Karman constant, whose value is 0.42, ' $C_s$ ' is Smagorinsky constant, ' $\delta$ ' is the distance to the closest wall, and ' $V$ ' is the volume of the computational cell. In this study, second order implicit discretization scheme is utilized, and in such a case, small positive numerical diffusions are generated. Therefore,  $C_s = 0.032$  is adopted that refers to LES using spectrum approach, which has no numerical diffusion.

## 2.2 Boundary conditions & Numerical Model

Shear stresses are specified for model and ground/embankment surface. When a wall-adjacent cell is in the laminar sub-layer, the wall shear stress is obtained from the laminar stress-strain relationship. If the mesh is too coarse to resolve the laminar sub-layer, it is assumed that the centroid of the wall-adjacent cells falls within the logarithmic region of the boundary layer, and the law-of-the-wall is employed that is stated as:

$$\frac{\bar{u}}{u_\tau} = \frac{\rho u_\tau y}{\mu}, \quad \frac{\bar{u}}{u_\tau} = \frac{1}{\kappa} \ln E \left( \frac{\rho u_\tau y}{\mu} \right) \quad \text{where } E = 9.8 \quad (4)$$

Finite volume method and structured collocated mesh approach are used for all the models. In the governing equations, second order central difference scheme is used for the convective and viscosity term discretization. Second order implicit scheme is used for the unsteady term. SIMPLE method, a semi-implicit approach, is used for solving the discretized equations in unstructured form. FLUENT 6.2 [9] have been used as the solver.

## 2.3 Aerodynamic Coefficients

Figure 1 shows the definition of aerodynamic forces. The aerodynamic coefficients can therefore be defined as follows:

$$C_D = \frac{D}{1/2 \rho U^2 H l} \quad (5)$$

$$C_L = \frac{L}{1/2 \rho U^2 H l} \quad (6)$$

$$C_p = \frac{p - p_{ref}}{1/2 \rho U^2} \quad (7)$$

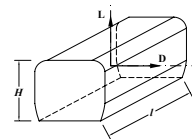


Figure 1. Definition of aerodynamic forces

where ' $p_{ref}$ ' is the reference pressure at mid point in span-wise direction of the lowest corner of the inlet boundary. ' $\rho$ ' is the reference density, and ' $U$ ' is the reference velocity that is taken at inlet for case 1 and 2 and is the velocity at a height of ' $3.23H$ ' above ground and a distance of ' $20H$ ' from inlet for case-3. The mean force and pressure coefficient is derived by taking average of the non-dimensional time ' $tU/H$ ' over 50 to 350.

## 2.4 Modeling Conditions and Cases

The height of the model ' $H$ ' is used as the characteristic dimension. The computational domain is extended to a distance of ' $30H$ ' from the model on all sides in  $xy$ -plane. A quasi-two-dimensional model is used to represent the middle car with span-wise length of ' $1.52H$ '. The Reynolds Number ' $Re$ ' is 10,000 for all simulations. The non-dimensional time step ' $tU/H$ ' is 0.04. Inlet boundary is specified as a uniform flow, outflow is specified at outlet boundary and symmetry conditions are applied for both sides. The upper/lower boundaries are also set as symmetry in case-1 whereas only the upper boundary is specified as symmetry for case-2 and case-3, as shown in Figure 2. Several models are used in this paper to understand the effect of attachment and embankment on the train aerodynamics. Table 1 provides detail for all these models.

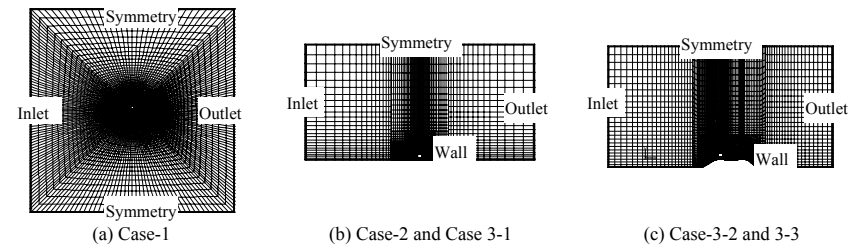


Figure 2. Numerical Domain with boundary conditions

Table 1 Model Detail		
Case	Sub-case	Description
1-Attachment Effect	1-1 Without Attachment	Basic rounded shape of the train.
	1-2 With Attachment	Train model with equivalent attachments area
2-Underbody Effect	2-1 Without space	Without any space between ground and attachment
	2-2 With space	A space of $0.06H$ between ground and attachment
3- Embankment Effect	3-0(a) Domain	Domain Only to simulate boundary layer
	3-0(b) Embankment	Embankment Only to simulate boundary layer
	3-1 On flat	Model (1-2) on flat surface
	3-2 Embankment (wind)	Model (1-2) on windward side of embankment
	3-3 Embankment (lee)	Model (1-2) on leeward side of embankment

## 3 NUMERICAL RESULTS

### 3.1 Effect of attachment

As discussed in section 1, most of the previous research did not consider attachment details, which are of great importance for the aerodynamic characteristics. To understand their importance, the experiment model [6] of the series-14 train middle car (Fig. 3 (a)) is considered. Case 1-1 (Fig. 3(b)) represents the basic shape of the train and case 1-2 (Fig. 3(c)) includes attachments are utilized. As the numerical model is quasi-two-dimensional, attachment details are provided keeping in view equivalent area in span-wise direction. The total attachment area is 20 % of basic train area.

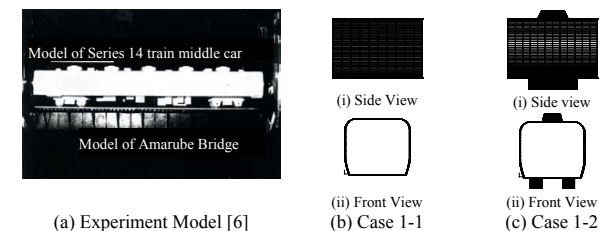


Figure 3. Numerical modeling of train geometry

Aerodynamic coefficients for the two cases are compared with experiment [6] in Figure 4(a). The drag has increased by nearly 50% with inclusion of attachments, which is more than the increase in area. Comparison with experimental results reveals that absence of attachments under-

estimates the drag whereas it overestimates the lift coefficient. Including attachments in train model provide good agreement for drag and better results for lift. Therefore, it is necessary to consider such attachments in numerical train model to obtain quantitative results.

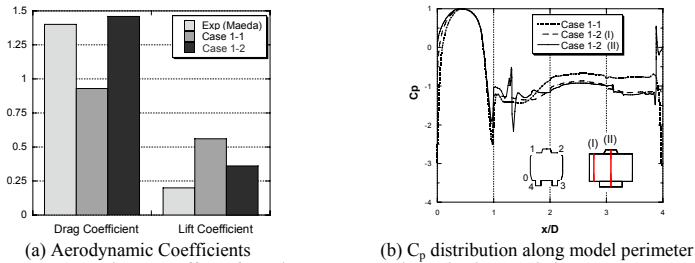


Figure 4. Effect of attachments on aerodynamic characteristics

Figure 4(b) shows the comparison of  $C_p$ -distribution on the model surface at the indicated section.  $C_p$ -distribution of section (I) of case 1-2 is affected with presence of attachment with reduction in pressure on leeside (2→3) and base (3→4) of the model. This causes the increase in drag and drop in lift. At section (II) a sudden rise in pressure followed by a drop takes place on the roof (1→2) because of the attachment whereas the base attachment develop a high pressure at its windward side with a steep drop in pressure on its leeside (3→4) that indicates flow separation. Comparing (I) and (II), it is evident that attachments not only have a strong localized effect, but they also influence the overall pressure distribution at other locations.

The instantaneous pressure contour for both cases is presented in Figure 5. For case 1-1 weak vortex shedding is observed with a narrow wake on the leeside that are away from the train model resulting in lesser negative pressure, whereas for the case 1-2 shedding is strong from attachments on roof and base and vortices occur close to the model with a wider wake. This results in greater negative pressure on the roof, base and lee-side increasing the drag while reducing the lift coefficient. Therefore, presence of attachments plays an important role in the formation and location of vortices. As lift is much dependent on the location of these vortices therefore a three-dimensional model with particular attachment details can further improve the results.

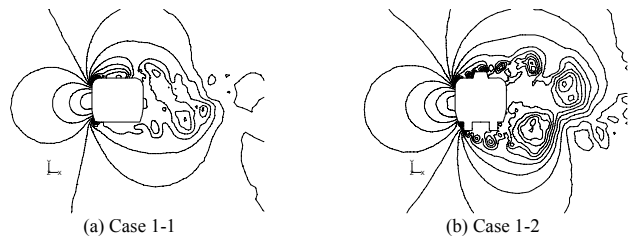


Figure 5. Instantaneous pressure contour indicating effect of attachment

### 3.2 Effect of Underbody flow

The underbody flow has a strong influence on the lift force acting on bluff bodies close to wall surfaces like trains on ground. Therefore this effect has to be appropriately modeled in the numerical domain. As the underbody attachments vary in length and height (Fig. 3(a)), for a quasi-

two-dimensional model easiest approach can be to provide a single representative attachment. As bogies and other attachments are very deep at particular sections, therefore in case 2-1 representative attachment is extended up to the ground and side openings are considered enough to simulate underbody flow. In case 2-2, a small space of 0.06H is provided underneath the attachment. Figure 6(a) shows that presence of even such small space below attachment causes a reduction of 70 % in lift. Figure 6(b) provides the  $C_p$ -distribution for both cases at mid-span. The pressure distribution is almost similar except for the high negative pressure under the attachment in case 2-2. In case 2-1 there is no suction under the attachment (3→4), which results in very high lift, whereas for case 2-2 the negative pressure under the attachment cause suction that reduces the net lift. A fractional difference in drag is because of drop in pressure on front face because of the jetting under the attachment. This comparison signifies the importance of underbody flow, and establishes that modeling of a small space between ground and train is necessary to get a true picture of the flow.

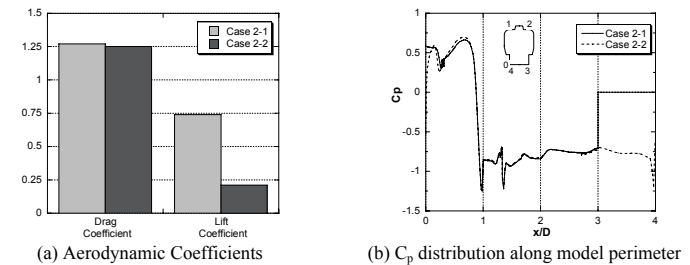


Figure 6. Effect of underbody flow on aerodynamic characteristics and pressure distribution

### 3.3 Effect of Embankment

Infrastructures are considered as critical section for train stability. The presence of such structures affects the boundary layer incident on train that modifies the flow pattern around the train. To understand how these structures influence the aerodynamic forces on trains, three cases are considered (case 3-1–3-3). The blockage is 5% for case 3-1 (flat ground) and 11 % for the case 3-2 & 3-3 (windward and leeward on embankment respectively). The height of embankment is '2H'. The effect of such a structure on boundary layer is first considered. Velocity profile at leading edge (L.E) of the train model in absence of train model is shown in Figure 7. For the case 3-1, there is no effect of boundary layer on the model as uniform velocity acts on the model. For the case 3-2 and 3-3, the incident velocity is not uniform therefore a reference velocity is required, which is selected at a distance of '20H' from the inlet and a height '3.23H' above the ground to have no influence from the inlet or the ground/embankment. This height refers to the mid-height of the model on embankment for the case 3-2 & 3-3. This reference velocity varies by less than 1% from the inlet velocity. Figure 8(a) shows an increase in drag force for case 3-2 and a drop for case 3-3 compared with case 3-1. Further, there is significant increase in lift force for both the cases on embankment. To understand the phenomena the mid-span  $C_p$  distribution is summarized (Fig. 8(b)), which indicates that in case 3-2 accelerated velocity (from embankment slope) in the lower frontal portion (0→1) of the model, increases pres-

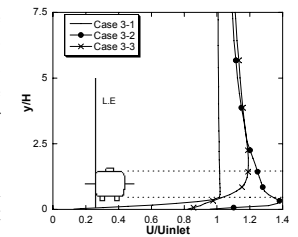


Figure 7. Boundary layer at leading edge

sure in that region. Moreover the combined effect of the embankment slope and train diverges the flow further away from leeside that causes higher negative pressure on the lee-face (2→3) of the model. The jetting in the underbody region (3→4) results in large negative pressure. For the case 3 -3, because of lesser velocity in lower portion of model the slope of  $C_p$  is mild as compared to case 3-1 (0→1). The train falls in the wake of the windward slope therefore the model experience lesser pressure, resulting in reduced drag force. A considerable increase in lift compared with case 3-1 is also observed due to the embankment.  $C_p$ -distribution indicate that pressure is nearly same for the three cases on the windward side of the base attachment (3→4), but the incident velocity is accelerated in case of embankment causing stronger jetting of the flow, which results in large pressure drop under the model. The instantaneous pressure contours (Fig. 9) show a large wake with vortices close to train model in case 3-2 and wake with vortices away from train model for case 3-3, which indicate weak vortex shedding in case 3-3.

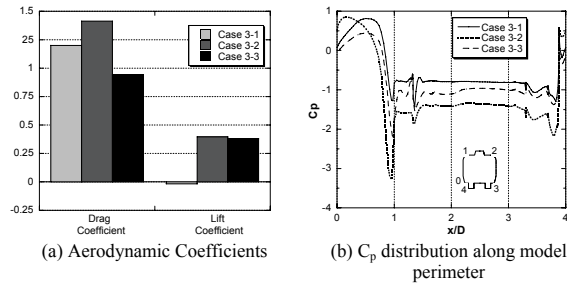


Figure 8. Effect of Embankment of Aerodynamic Characteristics

model are comparable with other models. This shows that LES is a good choice for the estimation of aerodynamic characteristics of trains and an appropriately modeled geometry can provide better estimation of forces.

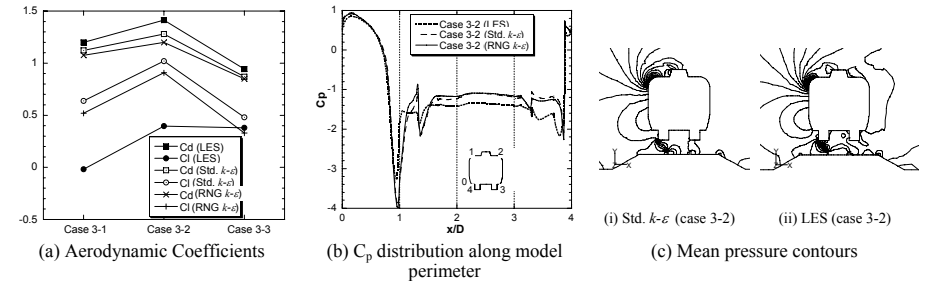


Figure 10. Comparison of aerodynamic characteristics of train on embankment using LES and  $k-\epsilon$  model

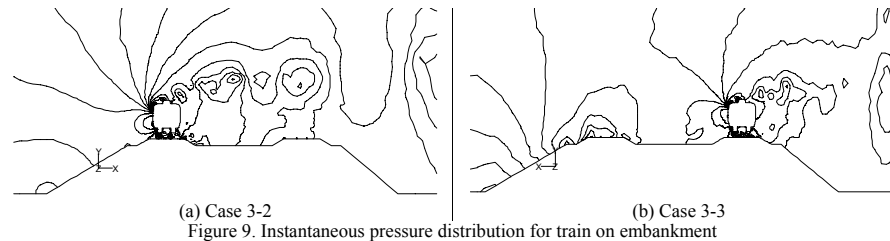
#### 4 CONCLUSION

In this study, LES turbulence model has been successfully used to quantitative prediction of aerodynamic characteristics of train in crosswind. The use of simplified train geometry does not provide quantitative results for aerodynamic coefficients and consideration of attachments is found necessary to obtain proper flow pattern and mechanism. Such attachments not only show a strong localized effect but also affect the overall pressure distribution. For realistic estimation of aerodynamic characteristics, proper modeling of underbody flow is found to be a key parameter.

In case of embankment the rise in velocity from the embankment slope increases the drag for the train on windward side whereas a drop in drag force occurs when model is on leeward side. This means that drag of trains on embankments can be reduced if they are designed to fall in the wake of the slope from both sides. Finally, a comparison of standard  $k-\epsilon$ , RNG  $k-\epsilon$  and LES model reveal that  $k-\epsilon$  models are not a good choice to capture the aerodynamic characteristics of trains because of the complex nature of flow resulting from attachments.

#### REFERENCES

- 1 M. Suzuki, K. Tanemoto, T. Maeda, Aerodynamic characteristics of train/vehicles due to cross-winds, J. Wind Eng. Ind. Aerodyn. 91 (2003) 209-218.
- 2 Chiu & Squire, An Experimental study of the flow over a train in a crosswind at large yaw angles up to 90°, J. Wind Eng. Ind. Aerodyn. 45 (1992) 47-74.
- 3 Chiu & Squire, A two-dimensional second-order vortex panel method for the flow in a crosswind over a train and other two-dimensional bluff bodies, J. Wind Eng. Ind. Aerodyn. 37 (1991) 43-64.
- 4 Chiu, Prediction of the aerodynamic loads on a railway trains in a crosswind at large yaw angles using an integrated two- and three-dimensional source/ vortex panel method, J. Wind Eng. Ind. Aerodyn. 57 (1995) 19-39.
- 5 Ishihara, Oka & Fujino, Numerical prediction of aerodynamic characteristics of a rectangular prism under uniform flow, J. Structural & Earthquake Eng., 62, No.1 (2006) 78-90. (In Japanese)
- 6 Tatsuo Maeda, Numerical Study of flow around car on bridge at crosswind conditions, RTRI Report Vol.4 No.2 '90. 2 (In Japanese).
- 7 W. Khier, M. Breuer, F. Durst, Flow structure around trains under side wind conditions: numerical study, Computers & Fluids 29 (2000) 179-195.
- 8 L. Cléon, P. Gautier, F. Sourget, High speed train operation and cross-winds: the DEUFRAKO programme, Revue Générale des Chemins de Fer – Juillet-août 2004 (In French)
- 9 Fluent Inc., FLUENT 6.2 Users Guide, 2005.



#### 3.4 Comparison of $k-\epsilon$ and LES

To investigate the pertinence of the  $k-\epsilon$  model for study of crosswind behaviour of trains, a comparison of the  $k-\epsilon$  and LES model is presented for the case of embankment effect. Figure 10(a) shows the aerodynamic coefficients based on the LES turbulence model along with standard  $k-\epsilon$  model and the RNG  $k-\epsilon$  model. For the drag coefficient, results of  $k-\epsilon$  models underestimate by not more than 15 % from LES. But for lift coefficient, variation is much larger in cases 3-1 & 3-2. Figure 10(b) displays the mid-span  $C_p$  distribution for the case 3-2 (windward), it can be seen that  $k-\epsilon$  models overestimates the negative pressure on the top corner of the model and it also amplify the effect of top attachment. Moreover, these models underestimate the pressure drop due to the underbody attachment, leading to overestimation of lift force. The mean pressure contours (Fig. 10(c)) from standard  $k-\epsilon$  and LES model for the case 3-2 indicates that the  $k-\epsilon$  model is not able to capture the pressure distribution in the attachment region on top as well as the bottom.

For the case 3-3, as the train lies in the wake of embankment slope, the approach velocity is much lesser that results in weak vortex shedding in underbody and leeside region of the train. Since this weak shedding has much less effect on mean pressure, therefore the results of LES